Materials Science & Technology

Seminar on Kesterites

Carolin Fella

Laboratory for Thin Films and Photovoltaics
Empa, Swiss Federal Laboratories for Materials Science and Technology
Überlandstr. 129, 8600 Dübendorf, Switzerland

Outline

- Motivation
- Basic properties
- Crystal structure and phases
- Defects/Doping
- Solar cells
- Limiting factors

Motivation

- High efficient chalcogen based technologies rely on elements which are rare or costly (e.g. In, Ga, Te)
- Requirements for an alternative:
  - direct band gap of 1…1.5 eV
  - long minority carrier lifetime – high mobility
  - low toxicity and abundant elements -> Cu_2ZnSnS_4 or $Cu_2ZnSnSe_4$ – I_2-II-IV-VI_4

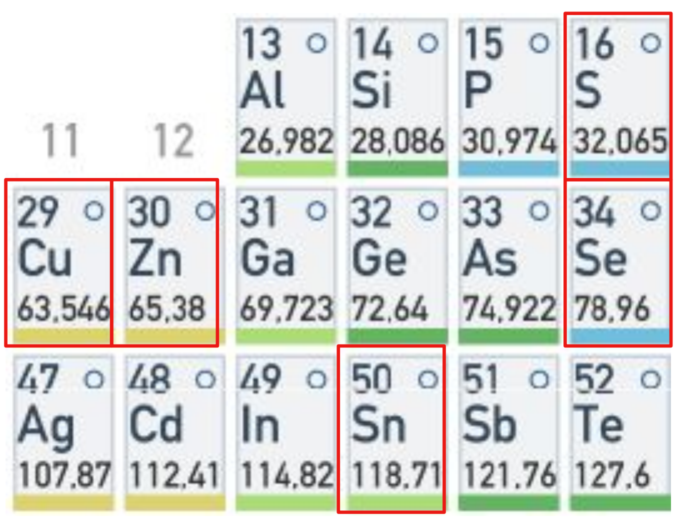

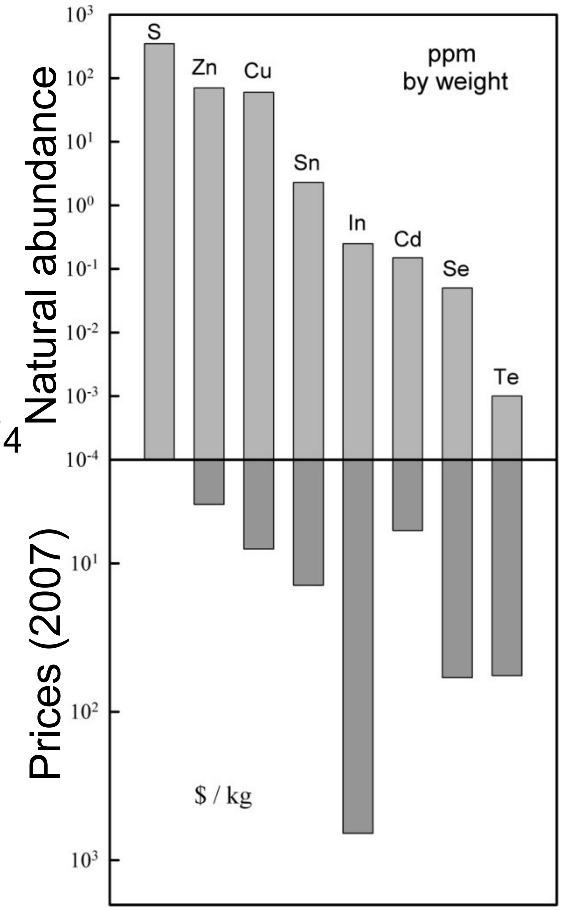

J. J. Scragg et al., phys. stat. sol. (b) **245**, No. 9, 1772 – 1778 (2008)

Material properties

- Direct band gap material
  E_g: CZTS ~ 1.5 eV & CZTSe ~ 1 eV[1]
  tunable band gap by combining S and Se
- Absorption coeff. ≥ 10^4 cm^{-1}
- Melting point of CZTSe: 805 °C[2]

[1] Chen et al., Crystal and electronic band structure of Cu2ZnSnX4 (X=S and Se) photovoltaic absorbers: First-principle insights, APL 94 (2009)
[2] H. Matsushita et al., Thermal analysis and synthesis from the melts of Cu-based quaternary Compounds Cu-III-IV-VI4 and Cu2-II-IV-VI4, Journal of Crystal Growth 208 (2000), 416

Crystal structure

IV Diamond

II - VI Zinc-blende

I - III - VI_2 Chalcopyrite

I_2 - II - IV - VI_4 Kesterite, Stannite

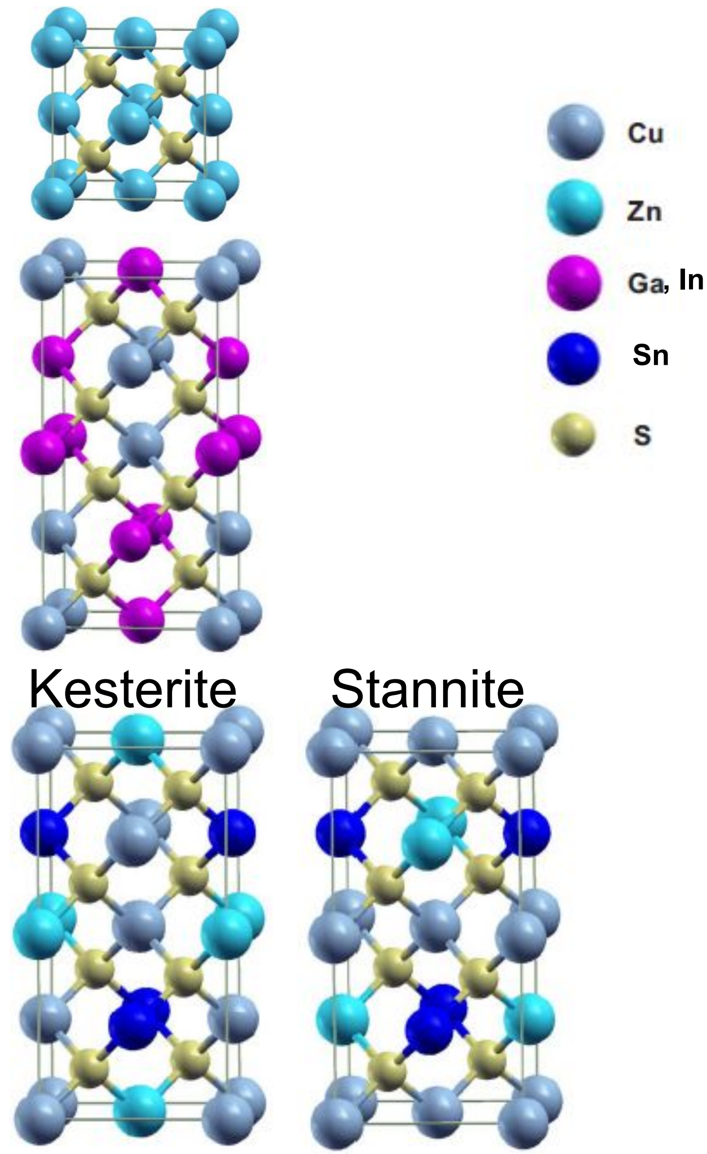

S. Chen, X. G. Gong, A. Walsh, S-H Wei, Electronic structure and stability of quaternary chalcogenide semiconductors derived from cation cross-substitution of II-VI and I-III-VI2 compounds, PHYSICAL REVIEW B 79, 165211 (2009)

Isothermal section of the Cu_2S – SnS_2 - ZnS

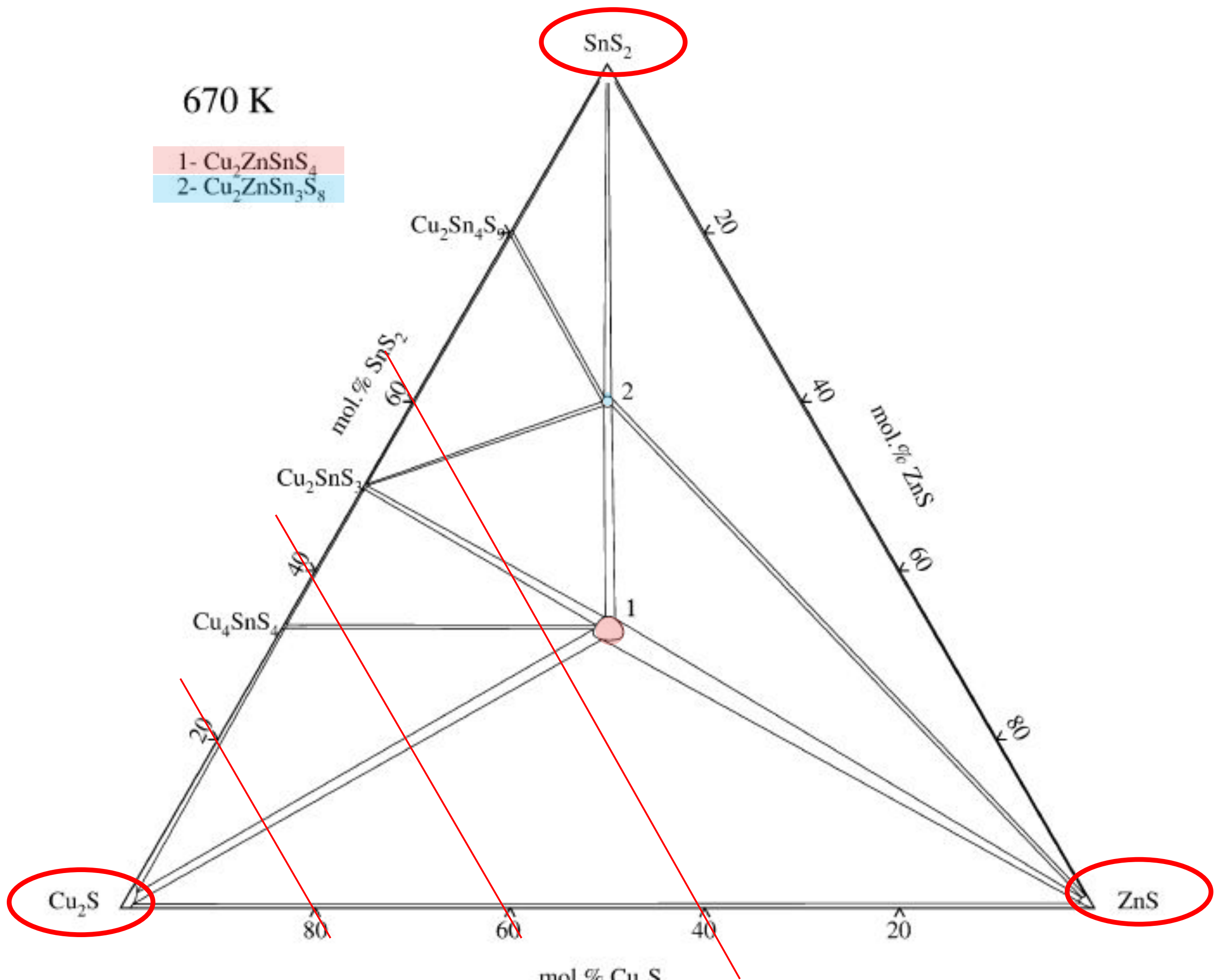

I.D. Olekseyuk, I.V. Dudchak, L.V. Piskach, Phase equilibria in the Cu2S–ZnS–SnS2 system, Journal of Alloys and Compounds 368 (2004) 135–143

Isothermal section of the Cu_2S – SnS_2 - ZnS

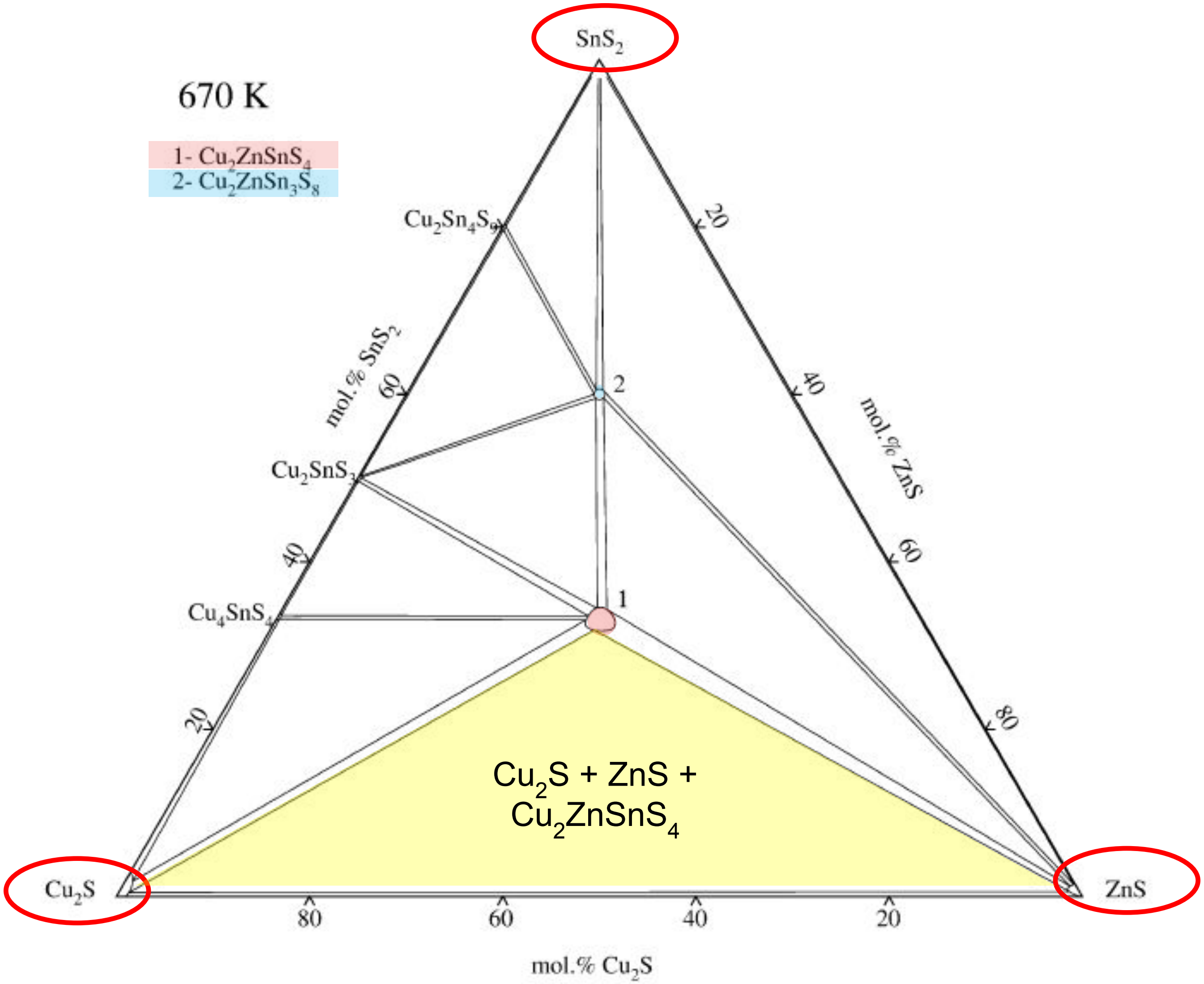

I.D. Olekseyuk, I.V. Dudchak, L.V. Piskach, Phase equilibria in the Cu2S–ZnS–SnS2 system, Journal of Alloys and Compounds 368 (2004) 135–143

Isothermal section of the Cu_2S – SnS_2 - ZnS

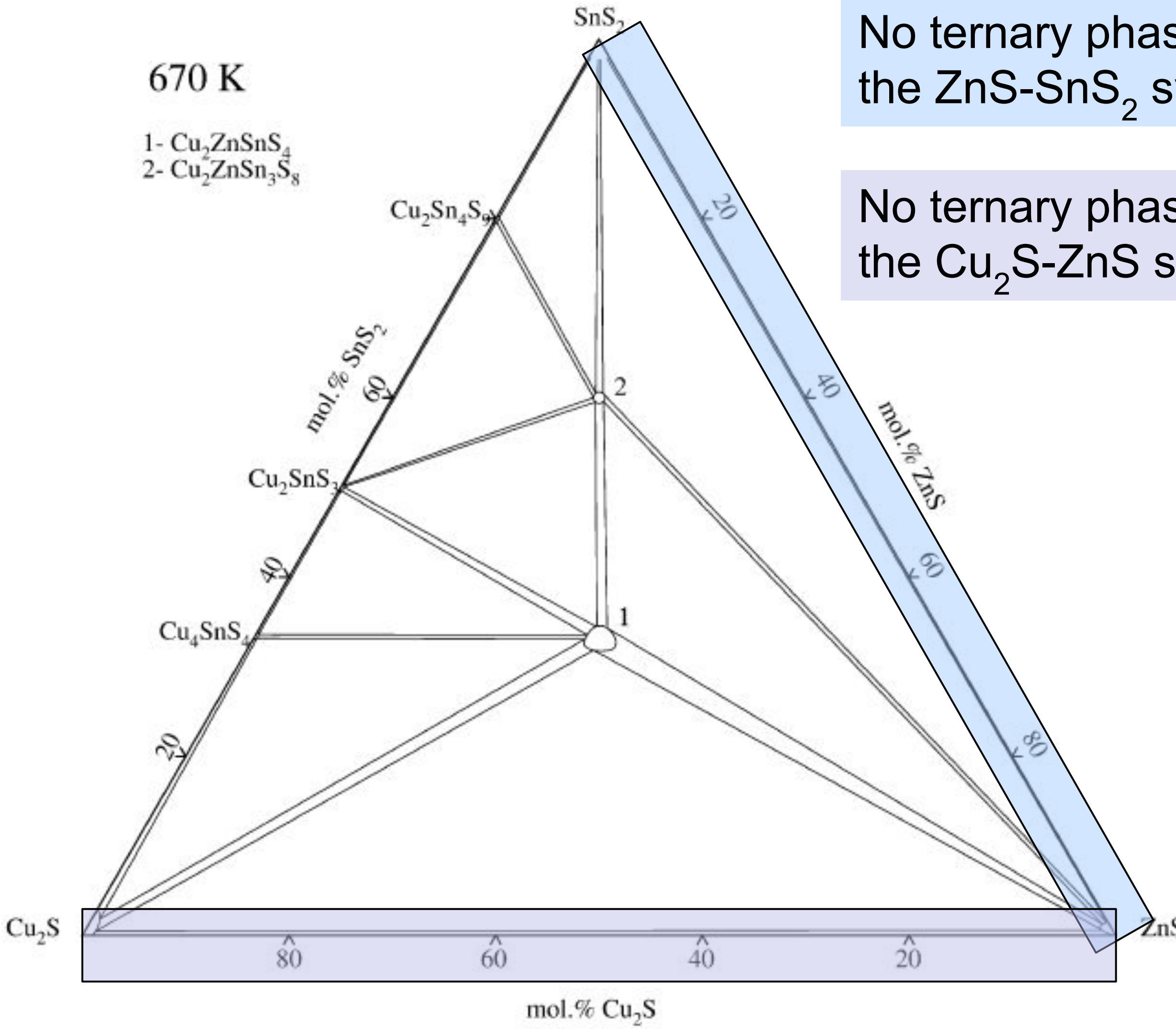

No ternary phases in the ZnS-SnS_2 system

No ternary phases in the Cu_2S-ZnS system

I.D. Olekseyuk, I.V. Dudchak, L.V. Piskach, Phase equilibria in the Cu2S–ZnS–SnS2 system, Journal of Alloys and Compounds 368 (2004) 135–143

Isothermal section of the Cu_2S – SnS_2 - ZnS

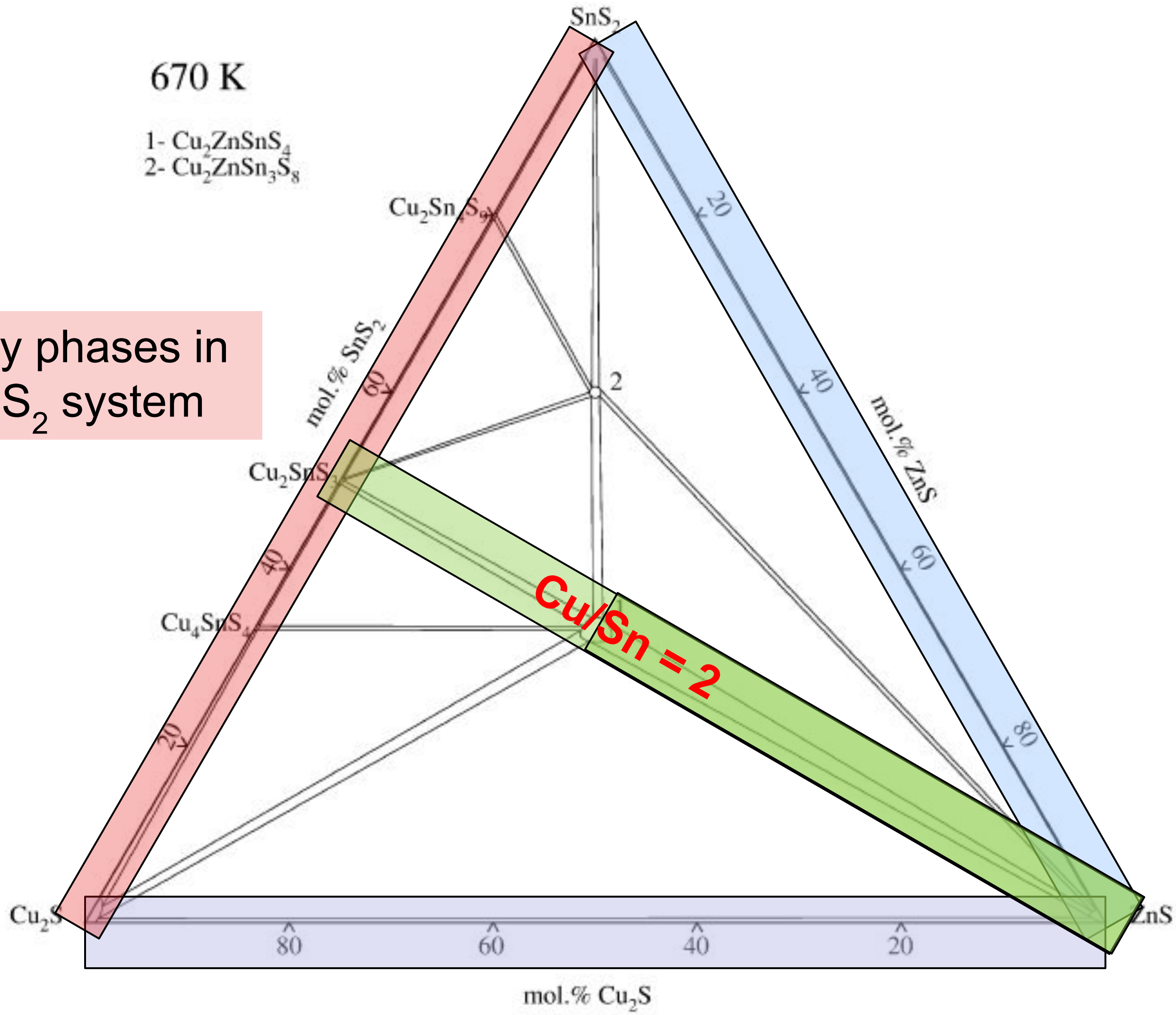

Some ternary phases in the Cu_2S-SnS_2 system

I.D. Olekseyuk, I.V. Dudchak, L.V. Piskach, Phase equilibria in the Cu2S–ZnS–SnS2 system, Journal of Alloys and Compounds 368 (2004) 135–143

- XRD

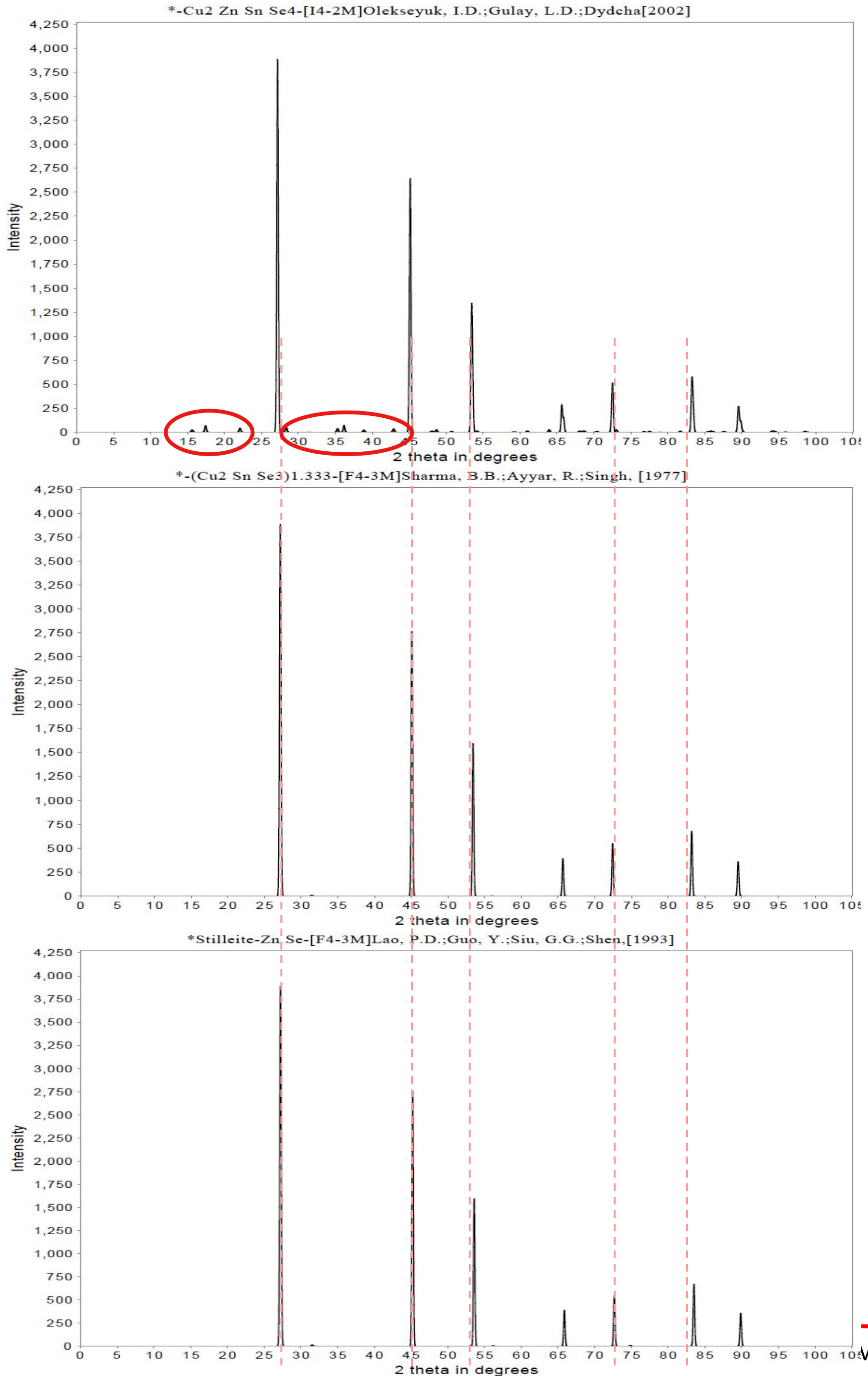

$Cu_2ZnSnSe_4$

Cu_2SnSe_3

ZnSe

Kesterite characterization

- XRD

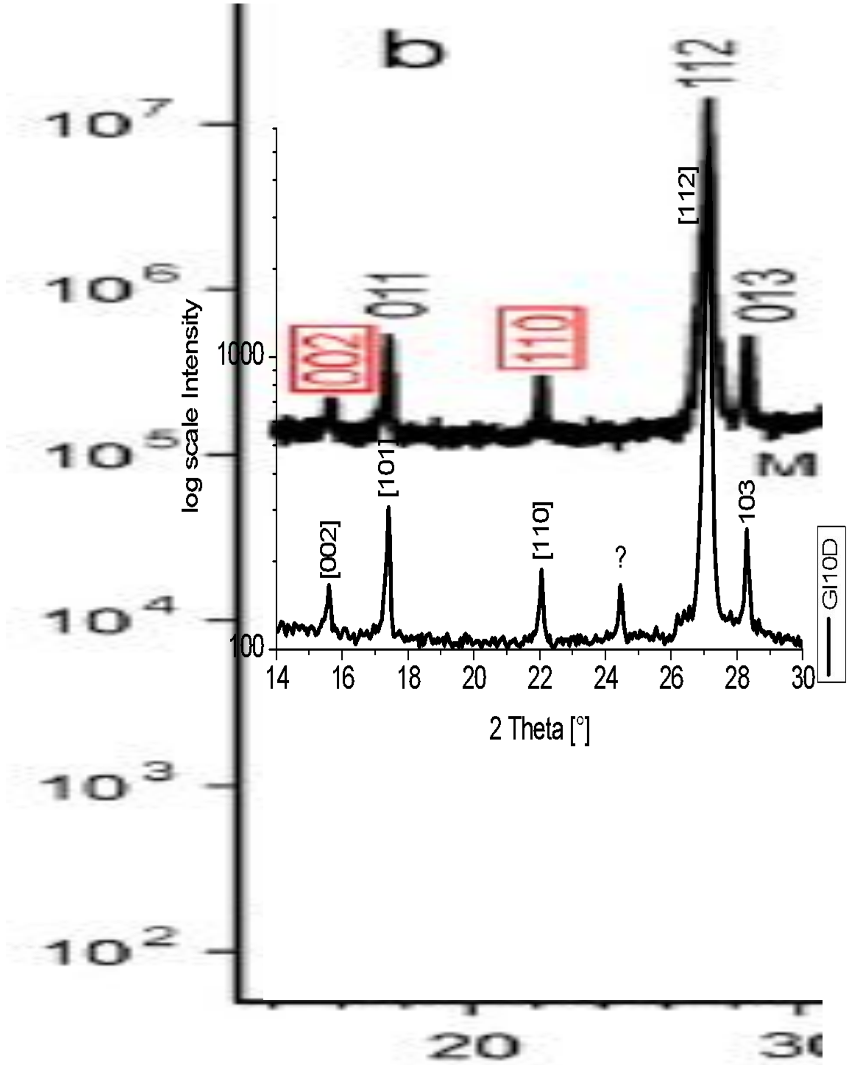

hydrazine processed CZTSSe

David B. Mitzi, Oki Gunawan, Teodor K. Todorov, Kejia Wang, Supratik Guha, The path towards a high-performance solution-processed kesterite solar cell, Sol. Energy Mater. Sol. Cells (2011)

Kesterite characterization

- Raman spectra for $Cu_2ZnSn(Se_{1-x}S_x)_4$

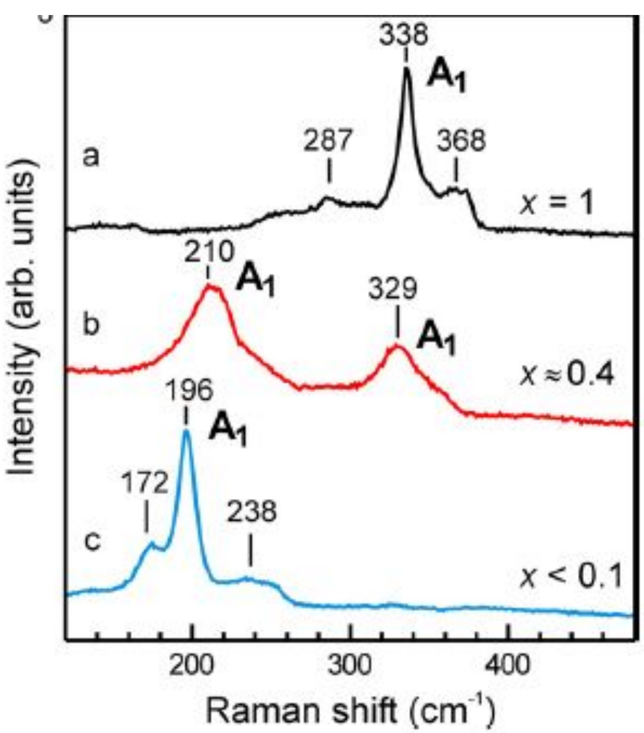

x = [S] / ([S]+[Se])

CZTS

≈ CZTSe

A_1 totally symmetric vibrations of the sulphur atoms alone

Stannite

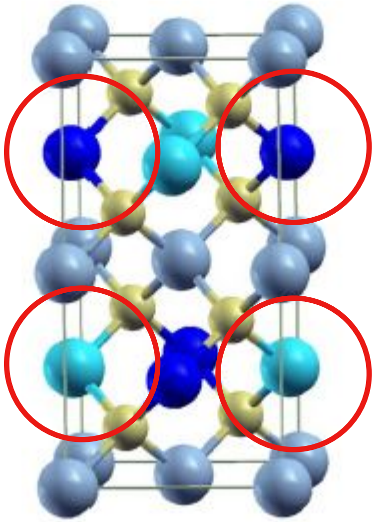

David B. Mitzi, Oki Gunawan, Teodor K. Todorov, Kejia Wang, Supratik Guha, The path towards a high-performance solution-processed kesterite solar cell, Sol. Energy Mater. Sol. Cells (2011)

Kesterite characterization

- Raman spectra for $Cu_2ZnSn(Se_{1-x}S_x)_4$

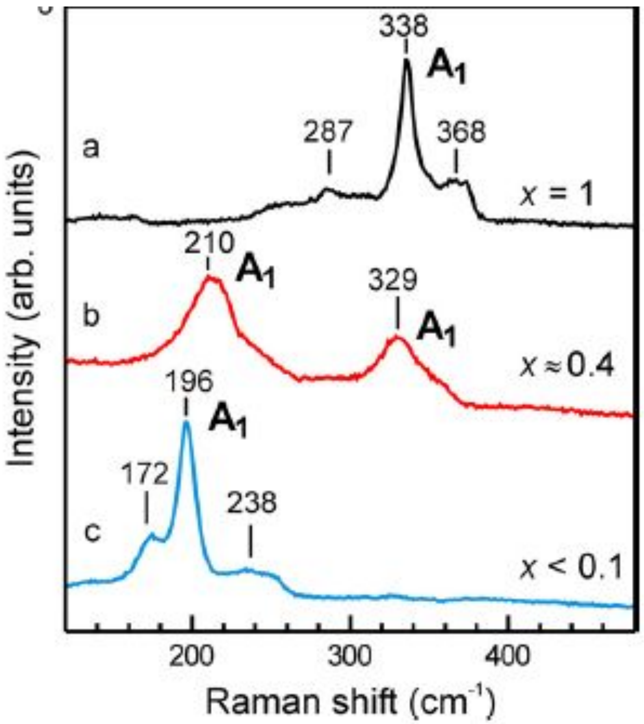

x = [S] / ([S]+[Se])

CZTS

≈ CZTSe

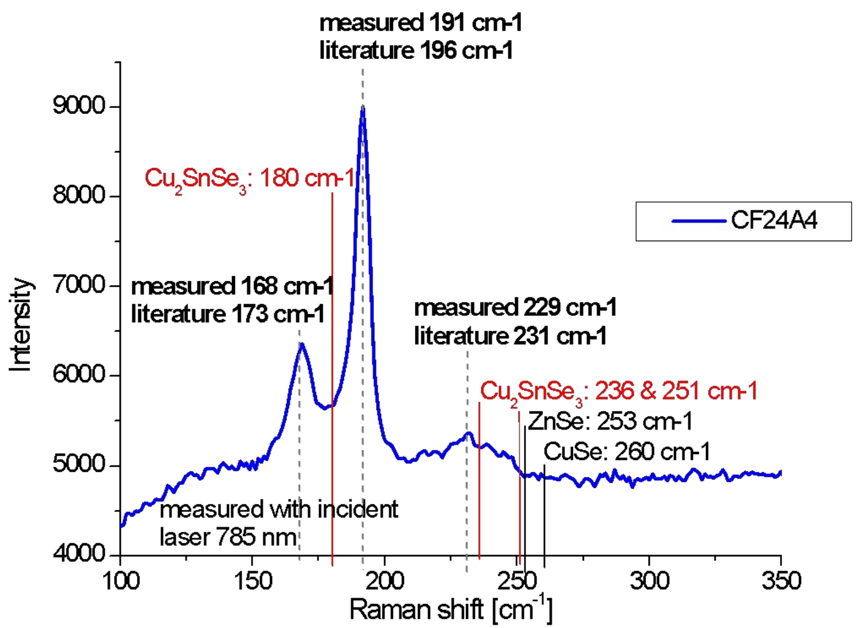

Reference: M. Altosaar et al., phys.stat.sol.a 205, No.1, 167-170 (2008)

David B. Mitzi, Oki Gunawan, Teodor K. Todorov, Kejia Wang, Supratik Guha, The path towards a high-performance solution-processed kesterite solar cell, Sol. Energy Mater. Sol. Cells (2011)

Electrical properties

Compound	Carrier density (p) [cm3]	Mobility (μ_h) [cm^2/Vs]	Resistivity [Ω cm]	Ref.	remarks
CIGS	2.00E+16	25	25	[1]	-
$Cu_2ZnSnSe_4$	2.00E+17	1.6	18	[2]	parameters depend strongly on Zn/Sn ratio
Cu_2ZnSnS_4	3.90E+16	30	5.4	[3]	slightly Zn-rich and Cu-poor film
Cu_2ZnSnS_4	8.00E+18	6	0.13	[4]	high carrier conc. might be due to the presence of CuS phase low hall mobility may result from the small grain size

[1] W. K. Metzger et al., Recombination kinetics and stability in polycrystalline Cu(In,Ga)Se2 solar cells, TSF 517 (2009)
[2] Wibowo et al., Pulsed layer deposition of quaternary Cu2ZnSnSe4 thin films, Phys. Status Solidi A 204 (2007)
[3] Liu et al., In situ growth of Cu2ZnSnS4 thin films by reactive magnetron co-sputtering, SOLMAT 94 (2010)
[4] T. Tanaka et al., Preparation of Cu2ZnSnS4 thin films by hybrid sputtering, J. Phys. Chem. Solids 66 (2005)

Intrinsic defects

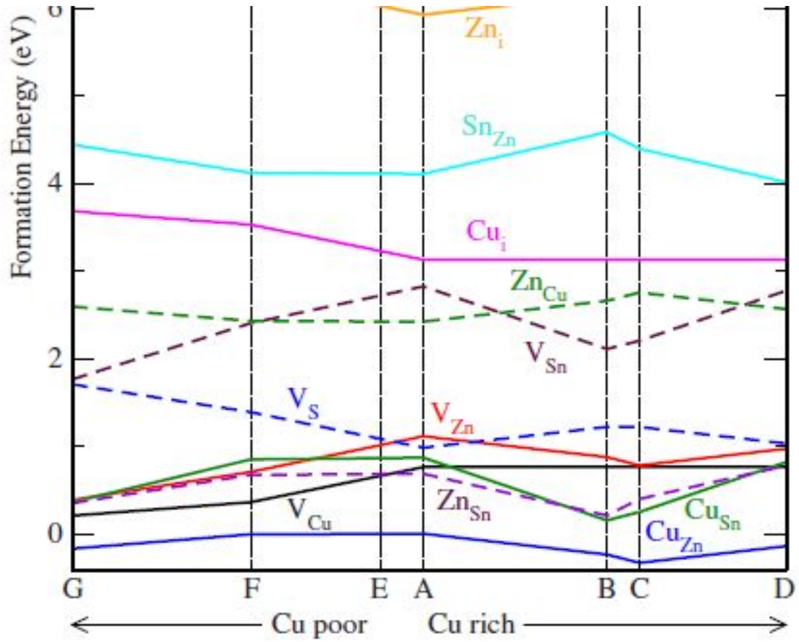

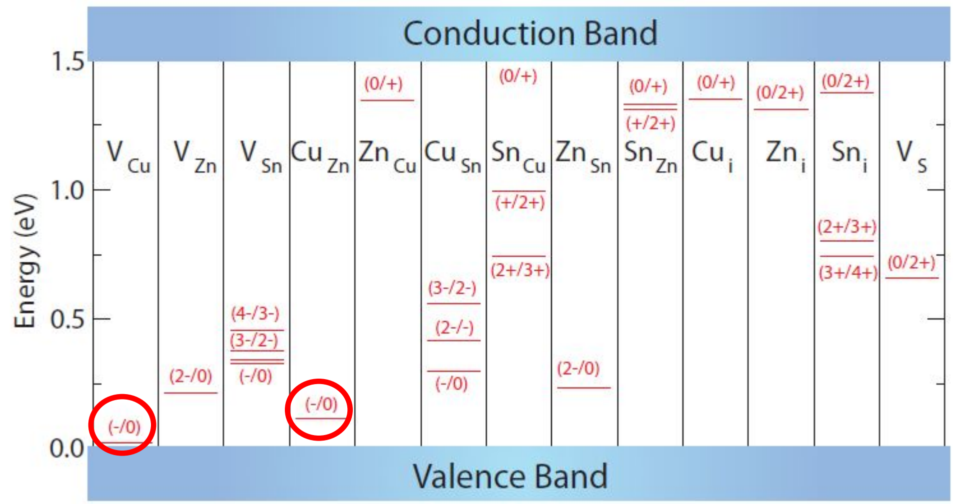

Calculated **transition energy levels**[2] of intrinsic defects in the band gap of Cu_2ZnSnS_4

	Cu-rich easy to grow pure CZTS	**Cu-poor** difficult to grow due to secondary phases
p-type	Cu_{Zn}	V_{Cu}
Transition energy level	deep acceptor 0.12 eV too deep, low p-type	shallow acceptor 0.02 eV easy to ionize, p-type

[1] Chen et al., Intrinsic point defects and complexes in the quaternary kesterite semiconductor Cu2ZnSnS4, Physical review B 81 (2010)
[2] Aron Walsh et al., Crystal structure and defect reactions in the kesterite solar cell absorber Cu2ZnSnS4 (CZTS): Theoretical insights

Defect complexes

- Role of electrically neutral defect complexes is predicted to be important, because they have remarkably low formation energies and electronically passivate deep levels in the band gap. E.g. $[Cu_{Zn}^{-} + Zn_{Cu}^{+}]^0$, $[V_{Cu}^{-} + Zn_{Cu}^{+}]^0$ and $[Zn_{Sn}^{2-} + 2Zn_{Cu}^{+}]^0$ may form easily in nonstoichiometric samples[2]

Complexes	$V_{Cu}+Zn_{Cu}$	$V_{Zn}+Sn_{Zn}$	$Cu_{Zn}+Zn_{Cu}$	$Cu_{Sn}+Sn_{Cu}$	$Zn_{Sn}+Sn_{Zn}$	$Zn_{Sn}+2Zn_{Cu}$	$Cu_{Zn}+Cu_i$	$Zn_{Sn}+Zn_i$
$\Delta H_{separated}$	3.10	5.13	2.43	7.41	4.80	5.55	3.24	6.71
ΔH_{int}	−2.35	−3.68	−2.22	−5.42	−3.94	−4.69	−2.25	−4.64
$\Delta H_{complex}$	0.75	1.45	0.21	1.99	0.86	0.86	0.98	2.08

2

- The antisite pair $[Cu_{Zn}^{-} + Zn_{Cu}^{+}]$ has the lowest formation energy i.e. this pair should have a high population in CZTS crystals[2]

- Formation of $[V_{Cu}^{-} + Zn_{Cu}^{+}]^0$ pair under Zn-rich/Cu-poor condition should be beneficial for maximizing solar cell performance[1]

- In poor quality films (like sputtered films) the formation energy of other complexes may decrease leading to other complex pairs

[1] Chen et al., Defect physics of the kesterite thin-film solar cell absorber CZTS, APL 96 (2010)
[2] Chen et al., Intrinsic point defects and complexes in the quaternary kesterite semiconductor Cu2ZnSnS4, Physical review B 81 (2010)

Compositional range for high Eff.

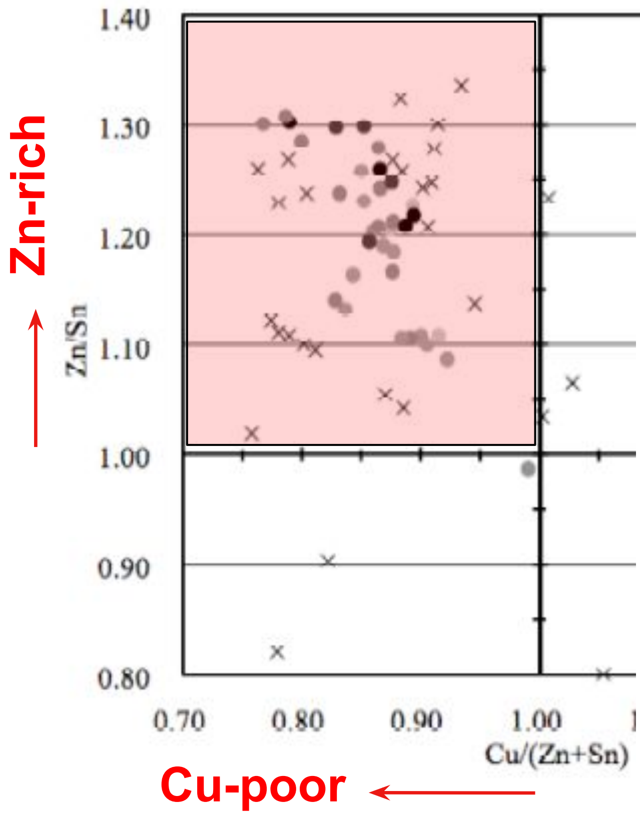

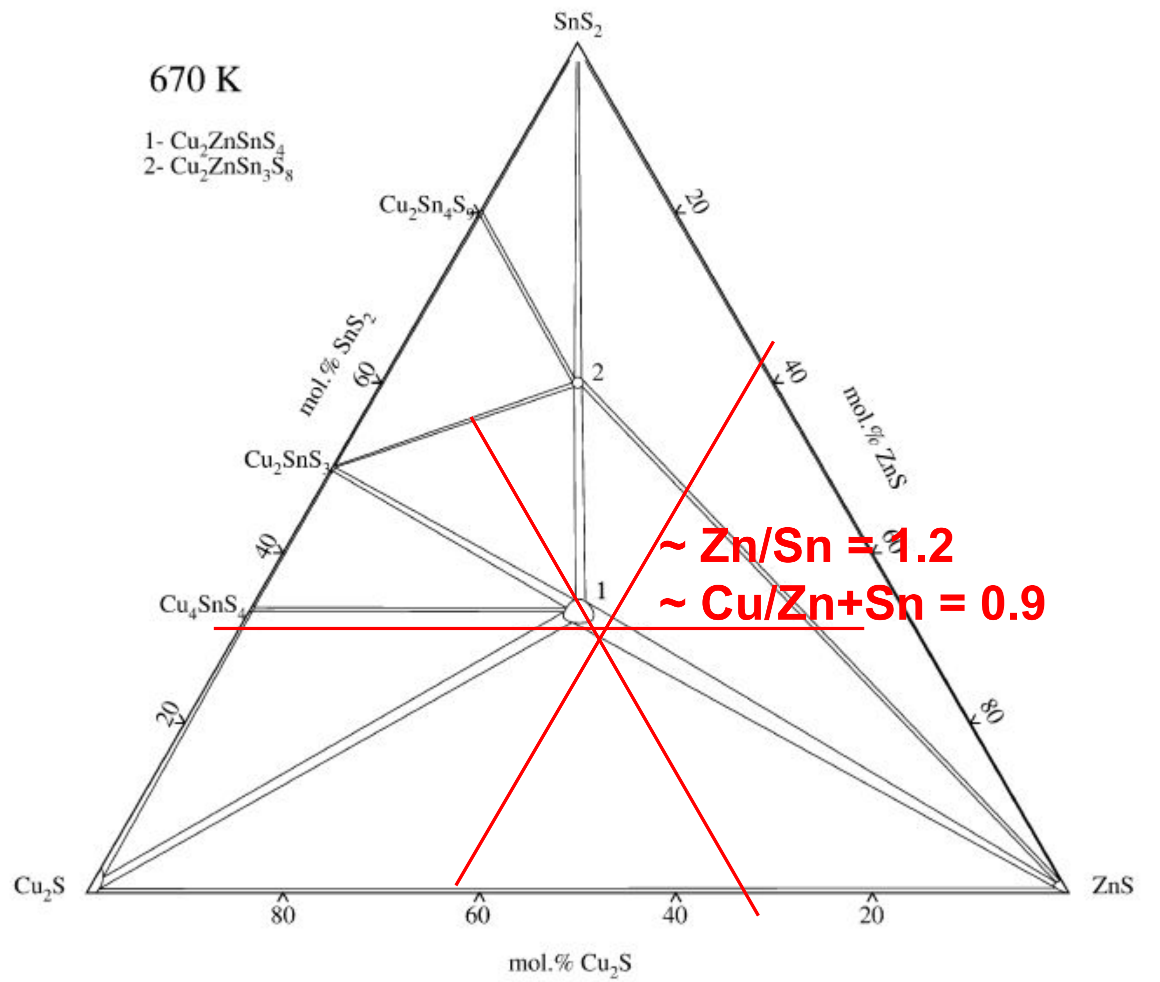

Hironori Katagiri, Kazuo Jimbo, Masami Tahara, Hideaki Araki and Koichiro Oishi, The influence of the composition ratio on CZTS-based thin film solar cells, Mater. Res. Soc. Symp. Proc. Vol. 1165, 2009

Solar cell structure

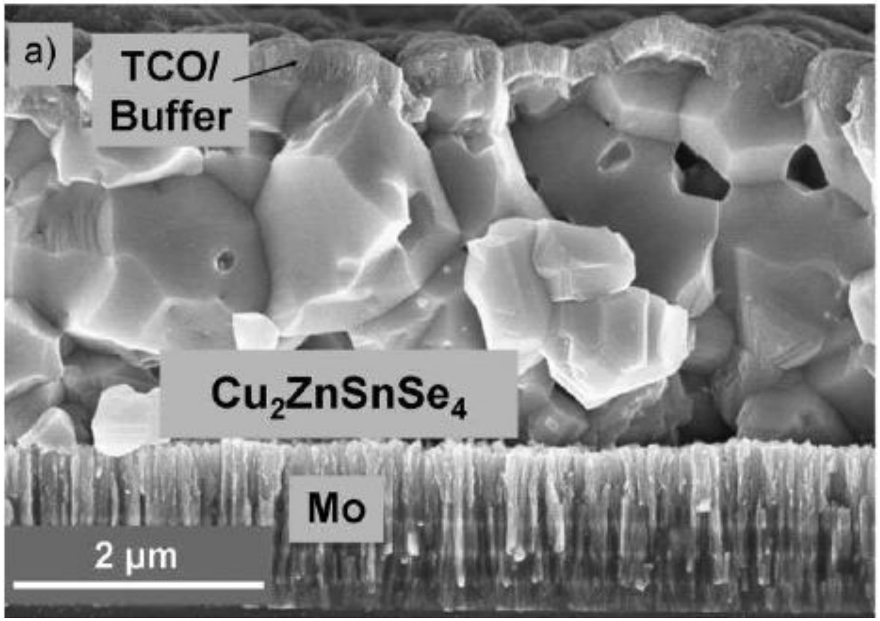

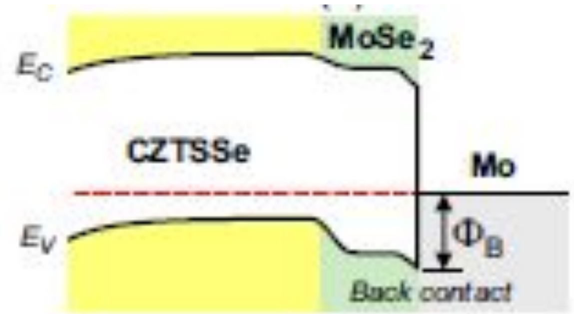

Hypothetical back contact band diagram, with blocking back contact[2]

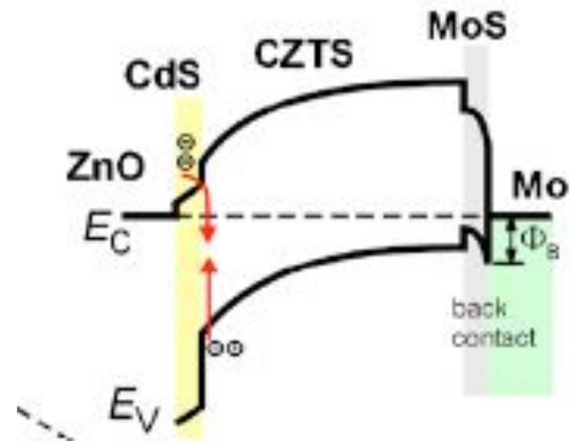

A hypothetical band diagram of a CZTS solar cell presenting a recombination path in the buffer/absorber interface and a back contact barrier[3]

[1]Teodor K. Todorov, Kathleen B. Reuter, and David B. Mitzi, High-Efficiency Solar Cell with Earth-Abundant Liquid-Processed Absorber, Adv. Mater. 2010, 22
[2] Oki Gunawan,a Teodor K. Todorov, and David B. Mitzi, Loss mechanisms in hydrazine-processed Cu2ZnSn(Se,S)4 solar cells, Appl. Phys. Lett. 97, 233506 (2010)
[3] K. Wang, O. Gunawan, T. Todorov, B. Shin, S. J. Chey, N. A. Bojarczuk, D. Mitzi, and S. Guha, Thermally evaporated Cu2ZnSnS4 solar cells, Appl. Phys. Lett. 97, 143508 (2010)

Deposition methods

- Vacuum

sputtering-based

CZTS: 6.77 % (Katagiri) – stacked metal sulfides Mo/Cu/SnS_2/ZnS (5 times)

CZTSe: 3.2 % (Zoppi) – stacked metals Mo/Cu/Zn/Sn

evaporation-based

CZTS: 6.8 % (Wang, IBM) co-evaporation from Cu, Zn, Sn, S sources

- Non-vacuum

electrodeposition

CZTS: 3.4 % (Ennaoui) – co-electrodeposition

Ink-based

CZTSSe: **9.7 %** (Todorov) – dissolved (CuS, SnS_2) and Solid (ZnS) chalcogenides in hydrazine

nanoparticles

CZTSSe: 7.2 % (Guo) – selenization of CZTS nanocrystals deposited by knife coating

Efficiency records

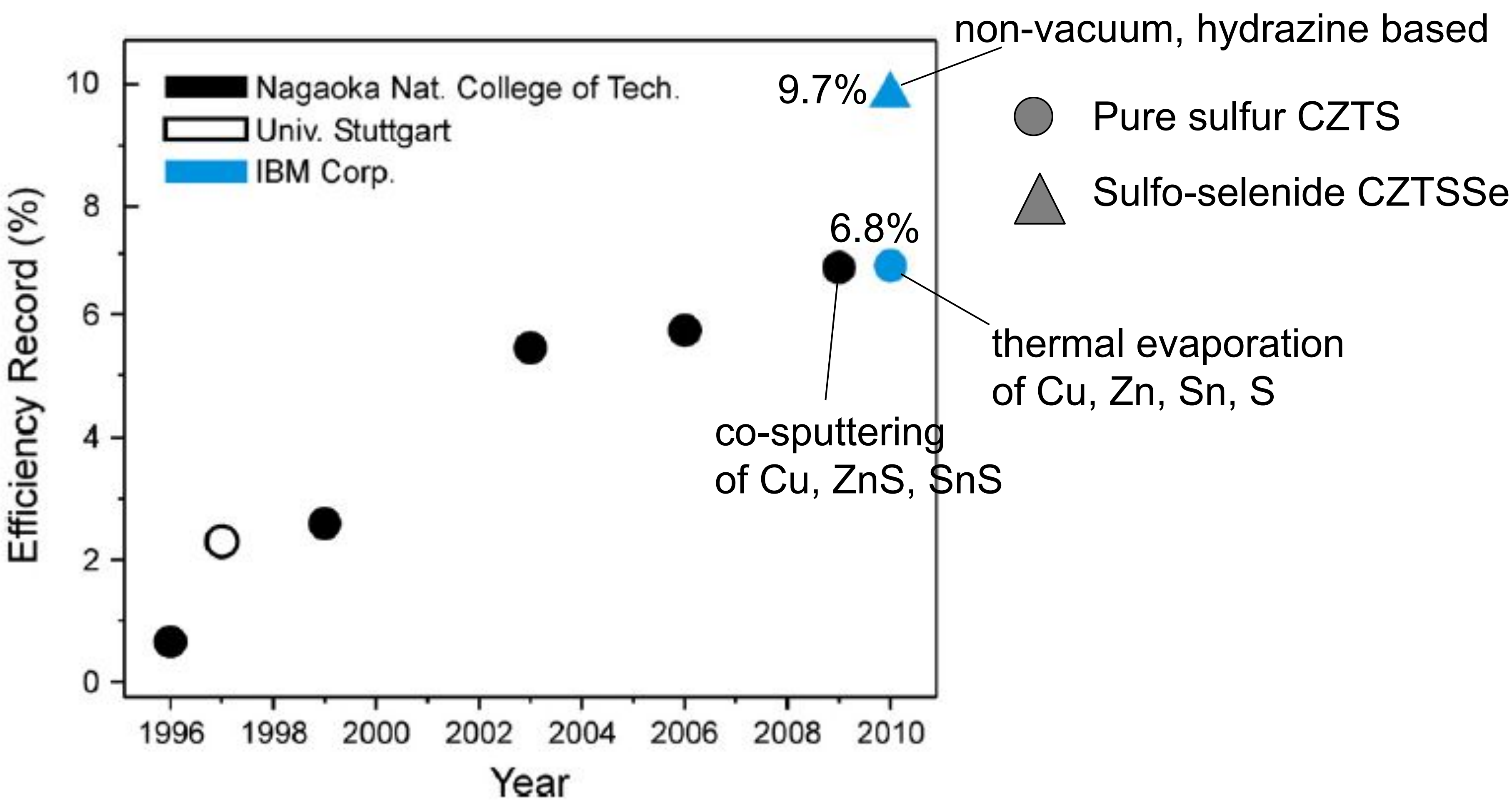

David B. Mitzi, Oki Gunawan, Teodor K. Todorov, Kejia Wang, Supratik Guha, The path towards a high-performance solution-processed kesterite solar cell, Sol. Energy Mater. Sol. Cells (2011)

Limiting factors[1]: effect on V_{oc}

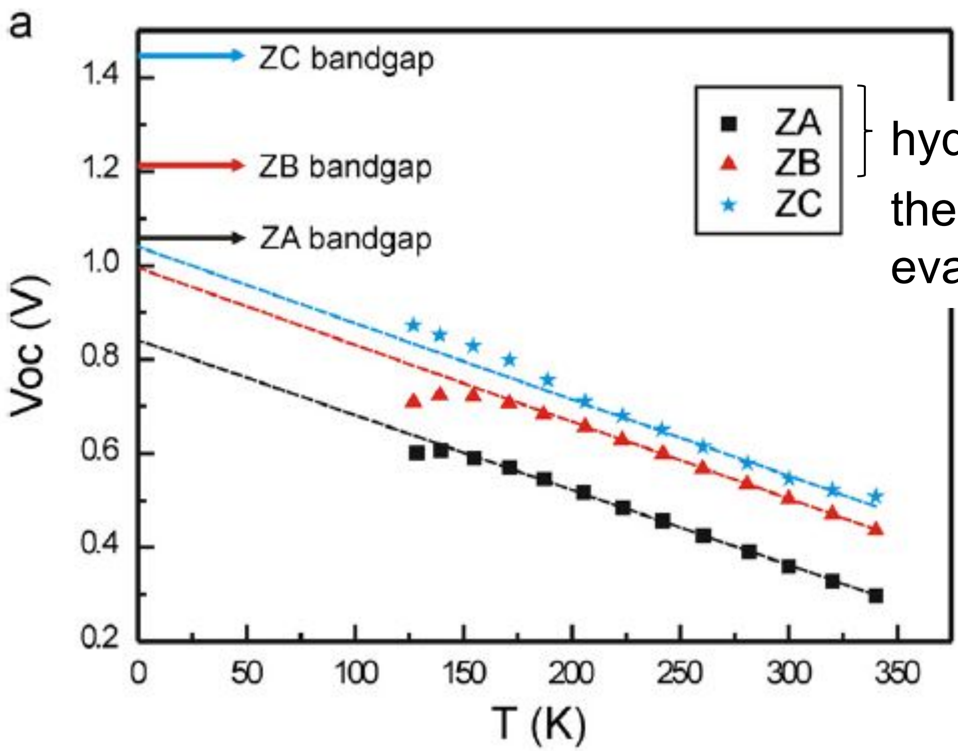

hydrazine-based

thermal co-evaporation

interface recombination

ZA: [S]/[S]+[Se] < 0.1 ⟶ E_g = 1.06 eV & E_A = 0.86 eV (η = 9.3%)

ZB: [S]/[S]+[Se] < 0.4 ⟶ E_g = 1.21 eV & E_A = 1.05 eV (η = 9.7%)

ZC: [S]/[S]+[Se] =1 ⟶ E_g = 1.45 eV & E_A = 0.96 eV (η = 6.8%)

[1] David B. Mitzi, Oki Gunawan, Teodor K. Todorov, Kejia Wang, Supratik Guha, The path towards a high-performance solution-processed kesterite solar cell, Sol. Energy Mater. Sol. Cells (2011)

Limiting factors[1]: effect of R_s on FF

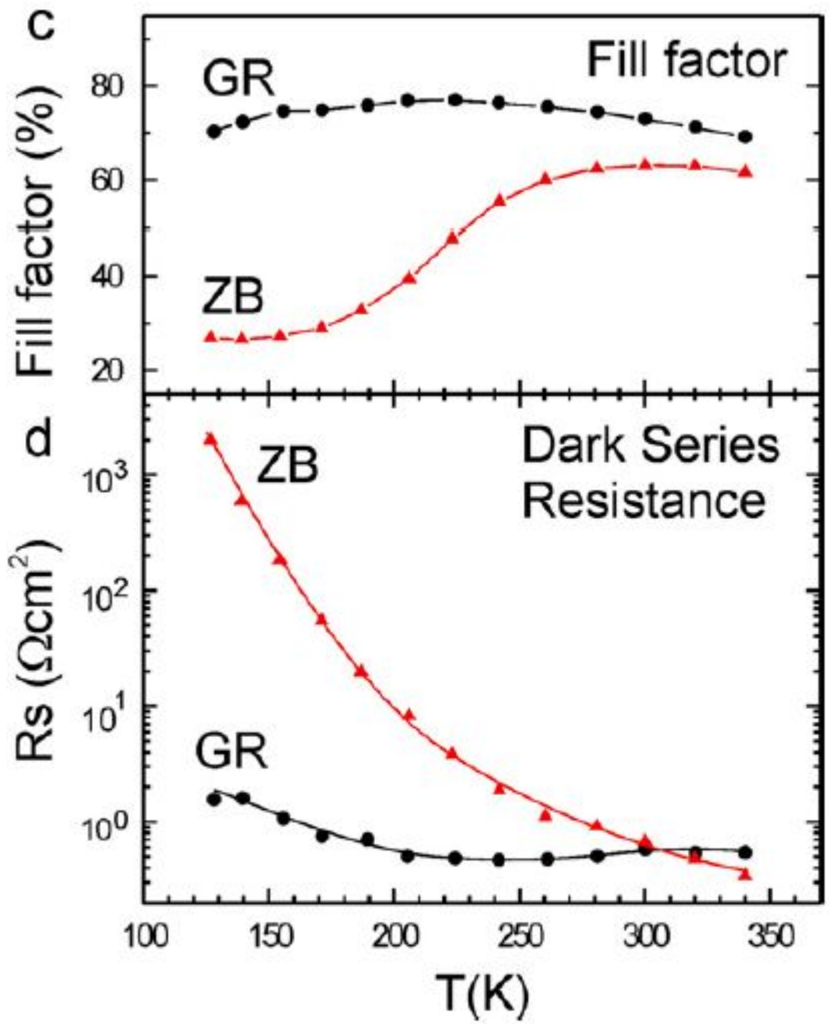

blocking back contact

ZB: [S]/[S]+[Se] < 0.4 ⟶ E_g = 1.21 eV & E_A = 1.05 eV (η = 9.7%)

[1] David B. Mitzi, Oki Gunawan, Teodor K. Todorov, Kejia Wang, Supratik Guha, The path towards a high-performance solution-processed kesterite solar cell, Sol. Energy Mater. Sol. Cells (2011)

Limiting factors[1]: effect on EQE

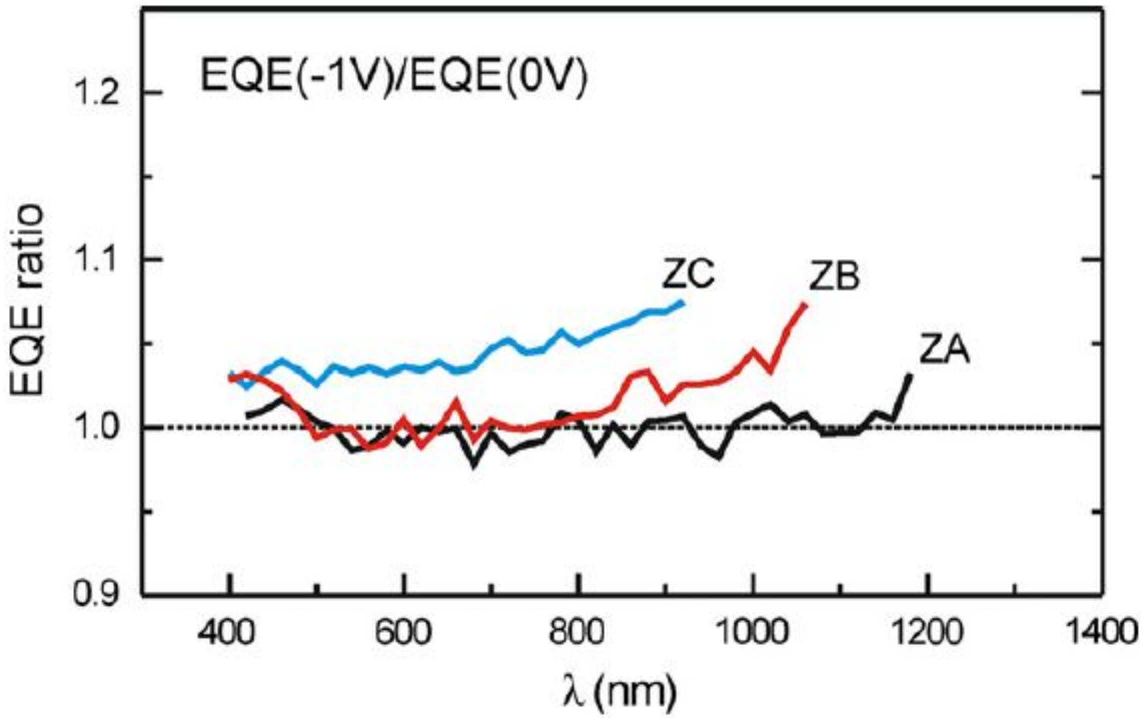

high defect density

ZA: [S]/[S]+[Se] < 0.1 ⟶ E_g = 1.06 eV & E_A = 0.86 eV (η = 9.3%)

ZB: [S]/[S]+[Se] < 0.4 ⟶ E_g = 1.21 eV & E_A = 1.05 eV (η = 9.7%)

ZC: [S]/[S]+[Se] =1 ⟶ E_g = 1.45 eV & E_A = 0.96 eV (η = 6.8%)

[1] David B. Mitzi, Oki Gunawan, Teodor K. Todorov, Kejia Wang, Supratik Guha, The path towards a high-performance solution-processed kesterite solar cell, Sol. Energy Mater. Sol. Cells (2011)

Conclusions

- Formation and identification of parasitic phases (Cu_2SnS_3, Cu_4SnS_4, ZnS)
- Metal ratio control: Cu-poor / Zn-rich important to control nature of electrical defects (Cu_{Zn}, V_{Cu} and defect complexes)
- Conventional Mo/CZTSSe/CdS/ZnO structure: 6.8% (by evaporation/ co-sputtering), 9.7% (based on hydrazine solutions)
- Limiting factors
  - V_{oc} (interface recombination)
  - R_s (blocking back contact)
  - EQE loss (short carrier lifetime, high defect density)

Thank you for your attention !

Back up sildes

CuS – ZnS – SnS phase diagram

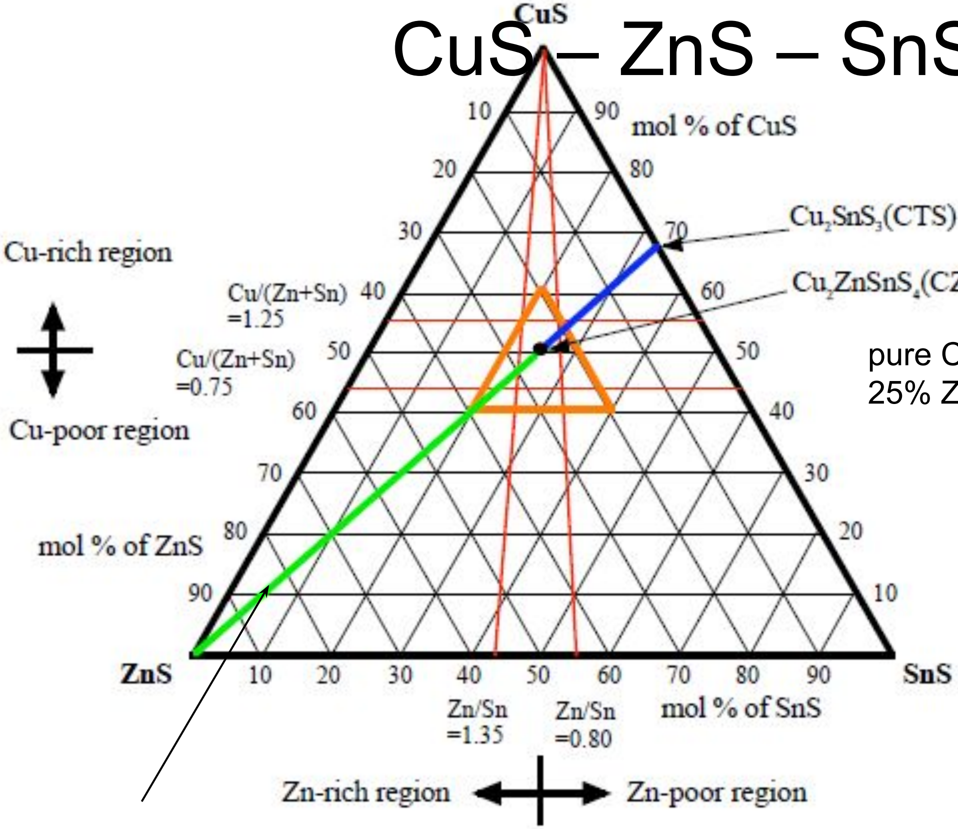

pure CZTS with 50% CuS, 25% ZnS and 25% SnS

High efficient solar cells exist only in a narrow composition range

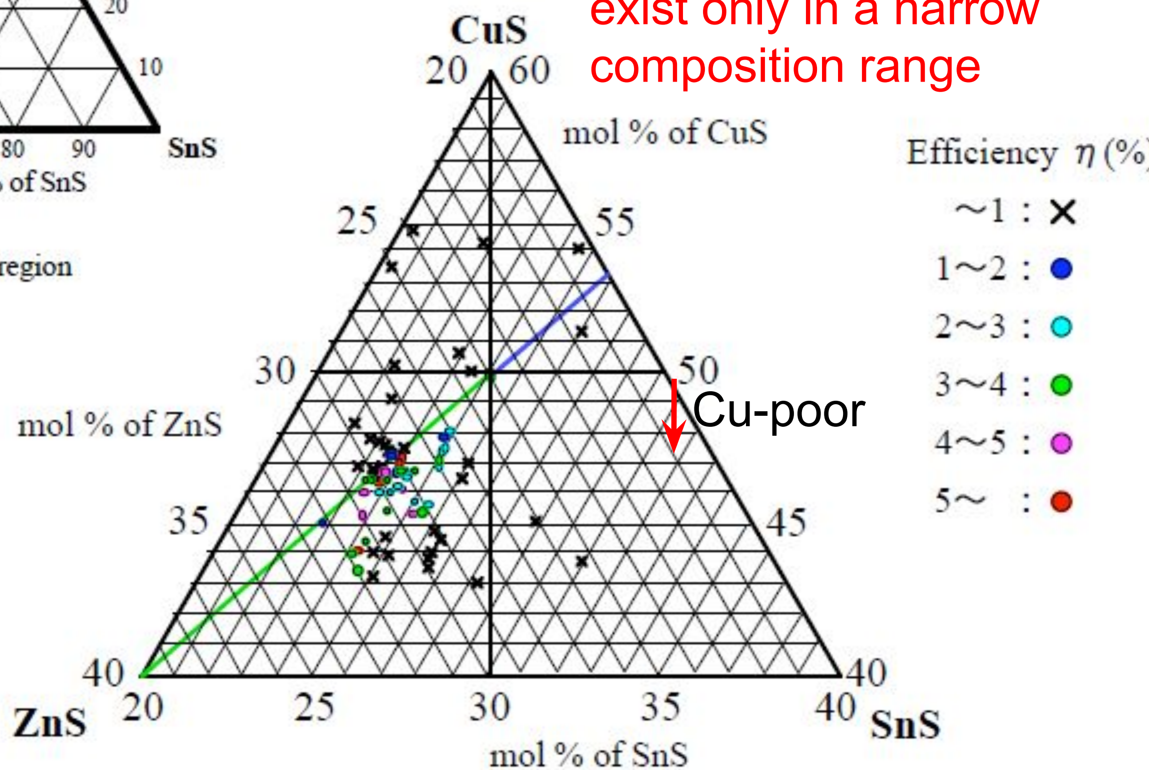

Katagiri et al., The influence of the composition ratio on CZTS-based thin film solar cells, Mater. Res. Soc. Symp. Proc. Vol. 1165 (2009)

Research overview

	Group		Material & Method			η [%]	Year
vac	K. Wang, Todorov	NY, US (IBM)	CZTS	thermal evaporation of Cu, Zn, Sn, S; annealing with presence of S	on Hp @540°C for 5min	6.8	2010
	H. Katagiri	Niigata, Japan	CZTS	three rf sources co-sputtering; targets: Cu, ZnS and SnS	sulfurization in N2+H2S (5%) at 580°C for 3h	6.8	2009
	H. Katagiri	Niigata, Japan	CZTS	co-evaporation of elemental Cu,Sn,S and binary ZnS	Tsub = 430-470°C; growth time 3h	5.7	2007
	B.-A. Schubert	Berlin,Germany (HZB)	CZTS	fast co-evaporation of ZnS, Sn, Cu and S for 16min;Cu-rich growth + KCN etching	Tsub = 550°C	4.1	2010
	K. Timmo	Tallinn, Estonia	CZTSSe	melt grown Cu2ZnSn(SxSe1-x)4 monograins (crystals with 50 um diameter)	evacuated quartz ampoules annealed to 1000K	7.8	2010/11
				from CuSe/S, ZnSe/S and SnSe/S in molten KI (potassium iodide)			
	G. Zoppi	Newcastle, UK	CZTSe	magnetron sputtered Cu(Zn,Sn); large number of alternate layers	selenization in Ar+elemental S at 500°C for 30min	3.2	2009
non	Q. Guo	Indiana, US	CZTSSe	selenization of CZTS nanocrystals deposited by knife coating	dried in air on HP@300°C then selenization at 500°C,20min	7.2	2010
vac	T. Todorov	NY, US (IBM)	CZTSSe	spin coating; Cu-Zn-Sn chalcogenide (S or Se) particle precursor in N2H4	annealing on Hp @ 540°C	9.7	2010
	K. Tanaka	Niigata, Japan	CZTS	spin coating; metal precursors dissolved in 2-methoxyethanol + MEA	annealing in N2+H2S (5%) @ 500°C for 1h	2	2010
	J. Scragg	Bath, UK	CZTS	ED of stacked elemental layers Cu/Sn/Cu/Zn	sulfurisation at 575°C for 2h	3.2	2010
	A. Ennaoui	Berlin, Germany	CZTS	ED of Cu-Zn-Sn precursors; co-electrodeposition	sulfurisation in Ar/H2S at 550°C for 2h	3.4	2009
	H. Araki	Niigata, Japan	CZTS	ED of Cu-Zn-Sn precursors for 20min	sulfurisation at 580 and 600°C for 2h	3.2	2009

Phase diagram of Cu_2S – SnS_2

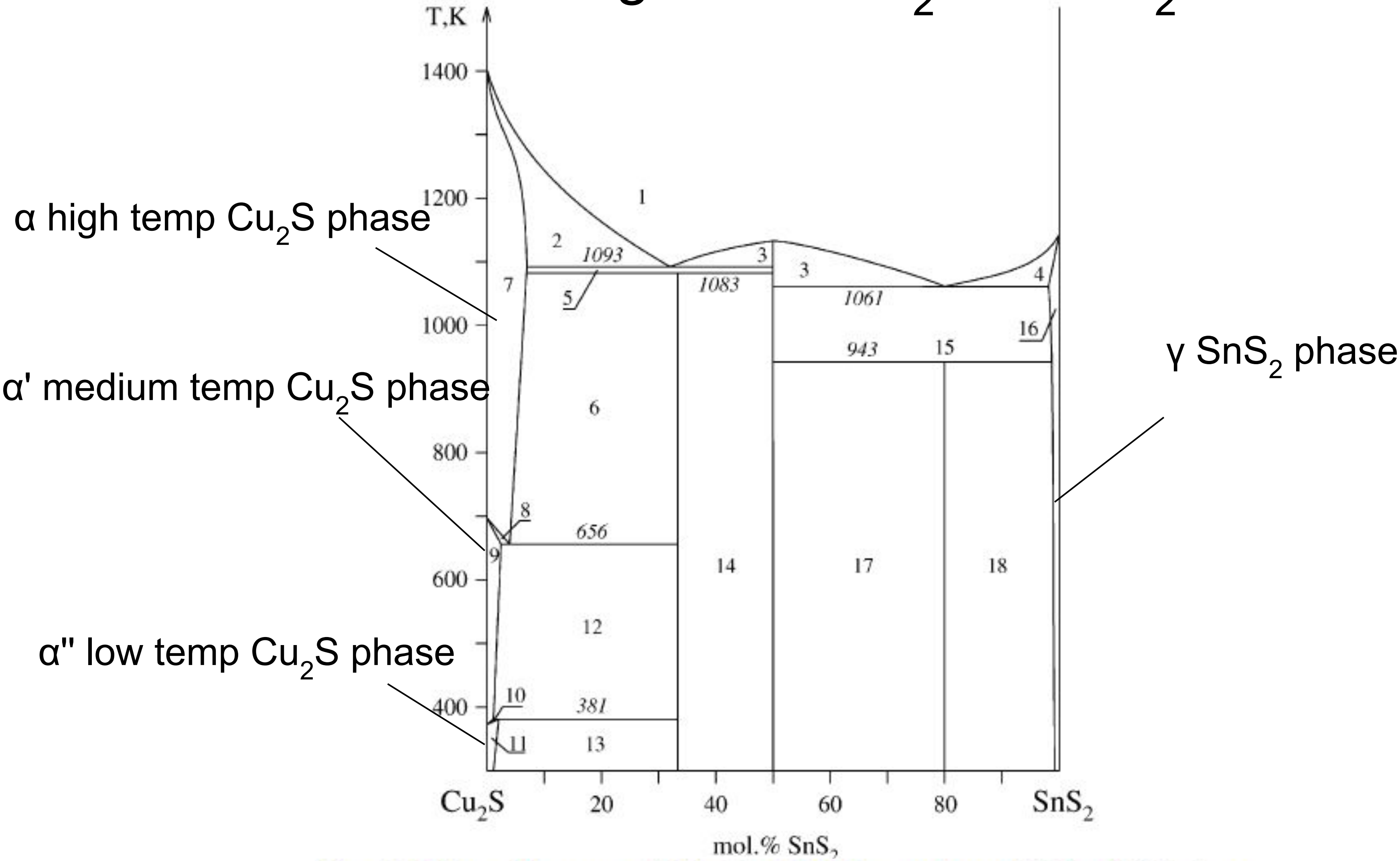

Fig. 2. Phase diagram of the Cu_2S–SnS_2 system: (1) L, (2) L + α, (3) L + Cu_2SnS_3, (4) L + γ, (5) Cu_2SnS_3 + α, (6) Cu_4SnS_4 + α, (7) α, (8) α + α′, (9) α′, (10) α′ + α″, (11) α″, (12) Cu_4SnS_4 + α′, (13) Cu_4SnS_4 + α″, (14) Cu_2SnS_3 + Cu_4SnS_4, (15) Cu_2SnS_3 + γ, (16) γ, (17) Cu_2SnS_3 + $Cu_2Sn_4S_9$, (18) $Cu_2Sn_4S_9$ + γ.

I.D. Olekseyuk, I.V. Dudchak, … ounds 368 (2004) 135–143

Phase diagram of Cu_2SnS_3 – Cu2ZnSnS4

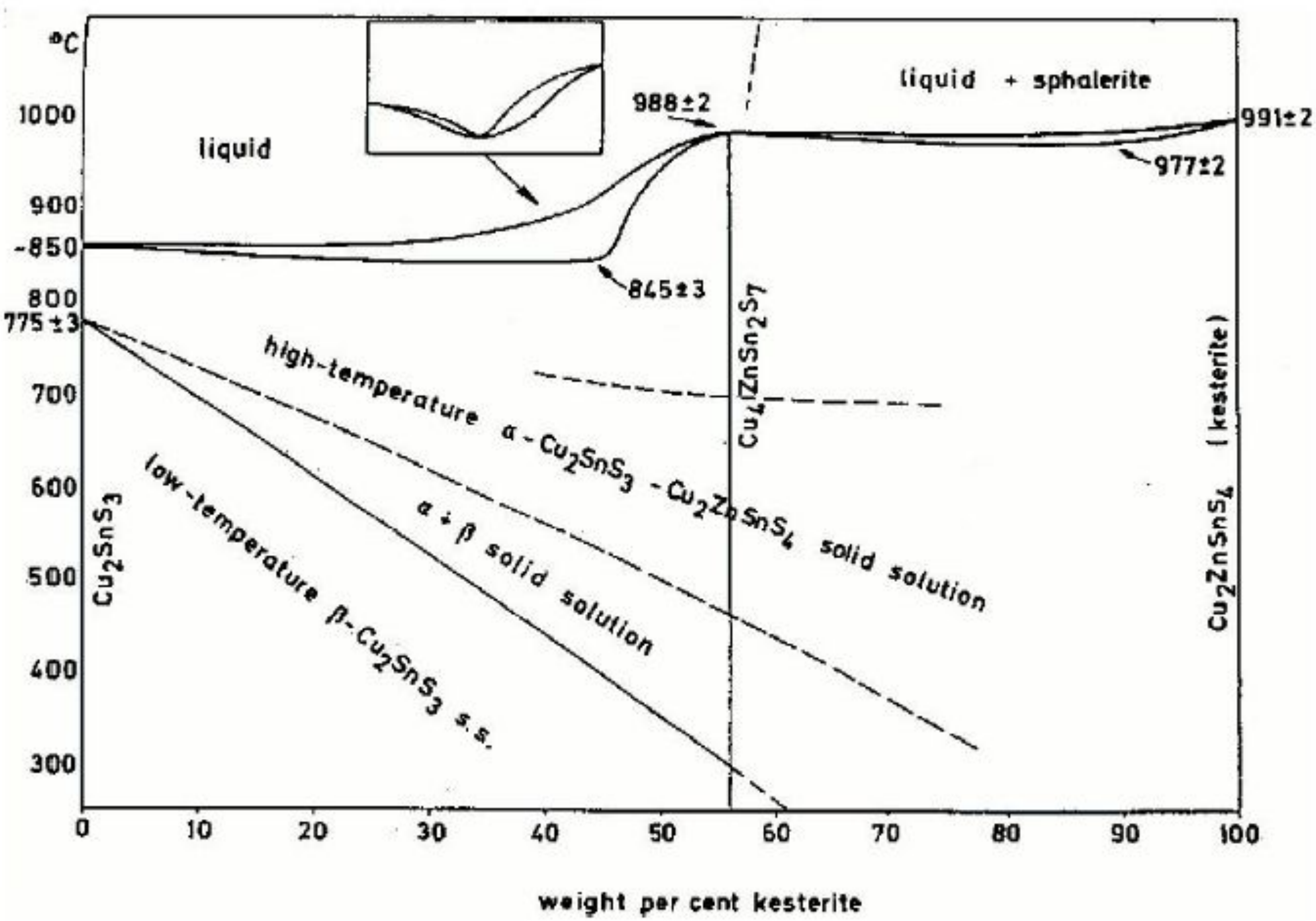

Cu_2SnS_3 is highly soluble in Cu_2ZnSnS_4

K. Roy-Choudhury, Neues Jahrbuch der Mineralogie, Monatshefte 9 (1974), S. 432-434.

Phase diagram of kesterite – sphalerite

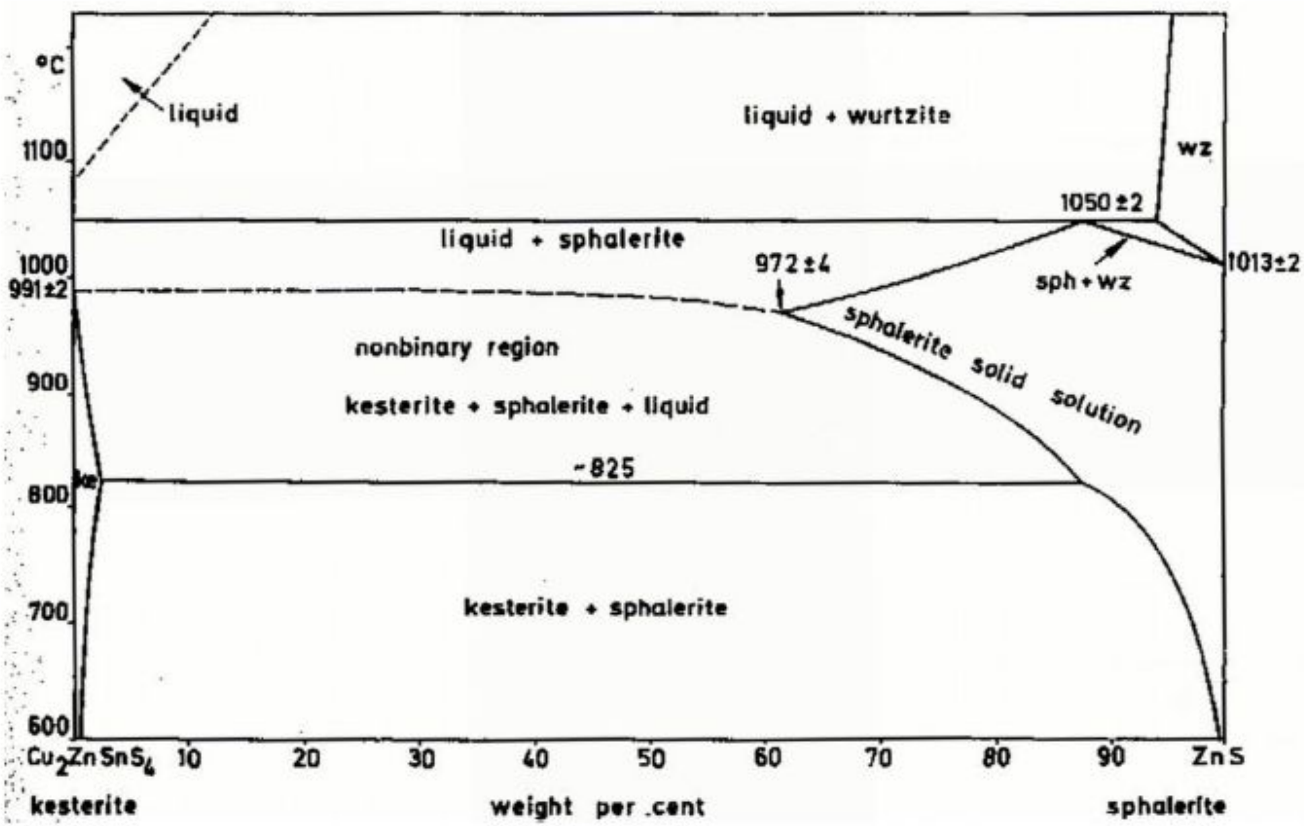

Very limited miscibility between Cu_2ZnSnS_4 and ZnS at elevated temperatures

G. Moh,Chemie der Erde 34 (1975), S. 1-59

Partial density of states

-> orbitals that determine the band gap of CZTSe are the VBM of antibonding Cu 3d and Se 4p / S 3p and the CBM of the antibonding Sn 5s and Se 4p / S 3p

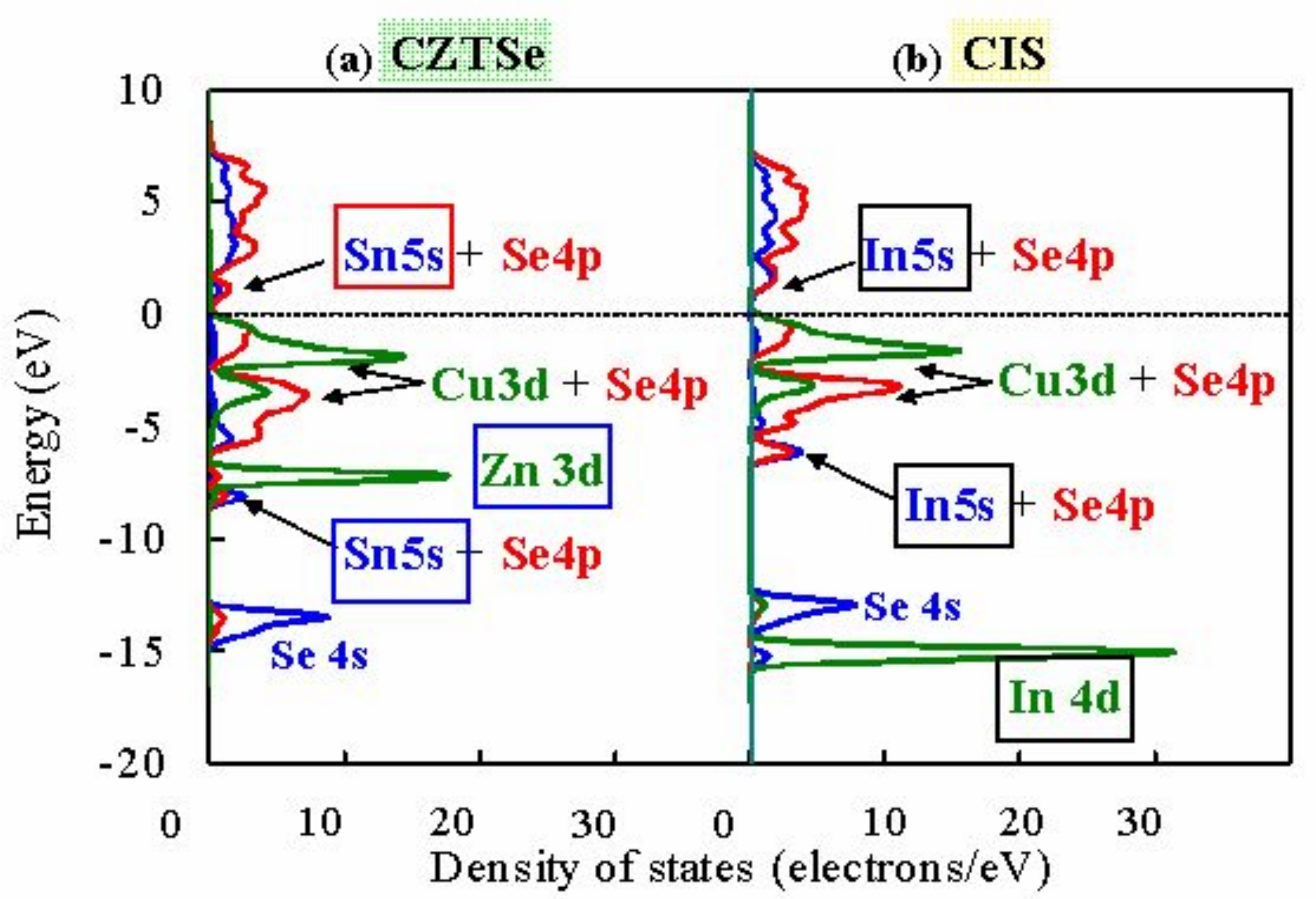

Nakamura et al., Electronic structure of stannite-type Cu2ZnSnSe4 by first principle calculations, Phys. Stat. Sol. C 6 (2009)

- XRD

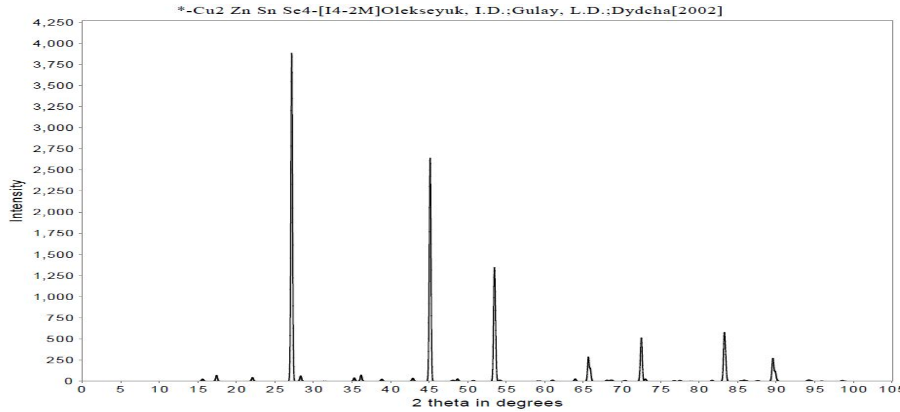

$Cu_2ZnSnSe_4$

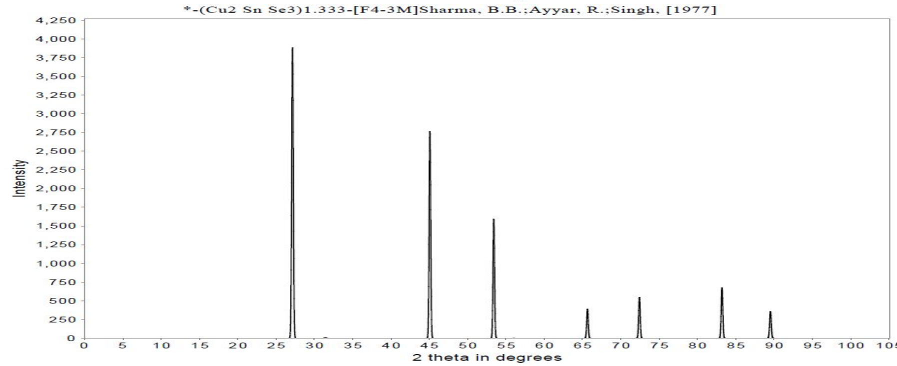

Cu_2SnSe_3

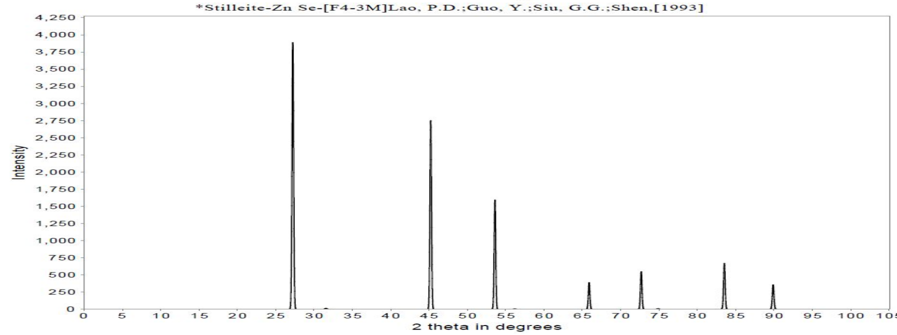

ZnSe

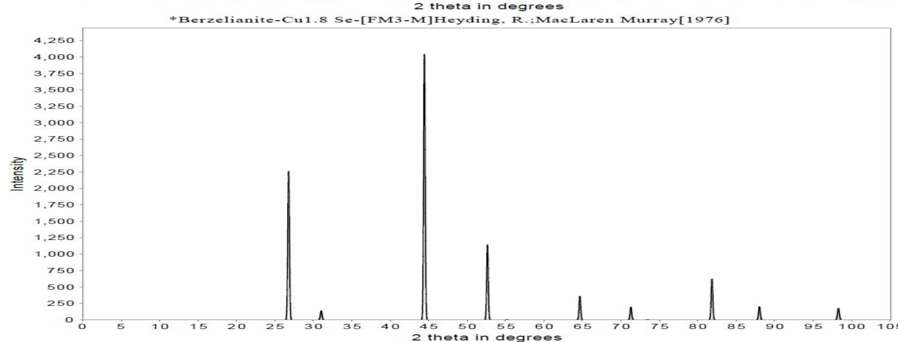

$Cu_{2-x}Se$